Letter

Measurement of the absolute branching fraction of the inclusive decay $\bar{\Lambda}_c^- \to \bar{n} + X$

M. Ablikim,[1] M. N. Achasov,[11,b] P. Adlarson,[70] M. Albrecht,[4] R. Aliberti,[31] A. Amoroso,[69a,69c] M. R. An,[35] Q. An,[66,53] X. H. Bai,[61] Y. Bai,[52] O. Bakina,[32] R. Baldini Ferroli,[26a] I. Balossino,[27a] Y. Ban,[42,g] V. Batozskaya,[1,40] D. Becker,[31] K. Begzsuren,[29] N. Berger,[31] M. Bertani,[26a] D. Bettoni,[27a] F. Bianchi,[69a,69c] J. Bloms,[63] A. Bortone,[69a,69c] I. Boyko,[32] R. A. Briere,[5] A. Brueggemann,[63] H. Cai,[71] X. Cai,[1,53] A. Calcaterra,[26a] G. F. Cao,[1,58] N. Cao,[1,58] S. A. Cetin,[57a] J. F. Chang,[1,53] W. L. Chang,[1,58] G. Chelkov,[32,a] C. Chen,[39] Chao Chen,[50] G. Chen,[1] H. S. Chen,[1,58] M. L. Chen,[1,53] S. J. Chen,[38] S. M. Chen,[56] T. Chen,[1] X. R. Chen,[28,58] X. T. Chen,[1] Y. B. Chen,[1,53] Z. J. Chen,[23,h] W. S. Cheng,[69c] S. K. Choi,[50] X. Chu,[39] G. Cibinetto,[27a] F. Cossio,[69c] J. J. Cui,[45] H. L. Dai,[1,53] J. P. Dai,[73] A. Dbeyssi,[17] R. E. de Boer,[4] D. Dedovich,[32] Z. Y. Deng,[1] A. Denig,[31] I. Denysenko,[32] M. Destefanis,[69a,69c] F. De Mori,[69a,69c] Y. Ding,[36] J. Dong,[1,53] L. Y. Dong,[1,58] M. Y. Dong,[1,53,58] X. Dong,[71] S. X. Du,[75] P. Egorov,[32,a] Y. L. Fan,[71] J. Fang,[1,53] S. S. Fang,[1,58] W. X. Fang,[1] Y. Fang,[1] R. Farinelli,[27a] L. Fava,[69b,69c] F. Feldbauer,[4] G. Felici,[26a] C. Q. Feng,[66,53] J. H. Feng,[54] K. Fischer,[64] M. Fritsch,[4] C. Fritzsch,[63] C. D. Fu,[1] H. Gao,[58] Y. N. Gao,[42,g] Yang Gao,[66,53] S. Garbolino,[69c] I. Garzia,[27a,27b] P. T. Ge,[71] Z. W. Ge,[38] C. Geng,[54] E. M. Gersabeck,[62] A. Gilman,[64] K. Goetzen,[12] L. Gong,[36] W. X. Gong,[1,53] W. Gradl,[31] M. Greco,[69a,69c] L. M. Gu,[38] M. H. Gu,[1,53] Y. T. Gu,[14] C. Y. Guan,[1,58] A. Q. Guo,[28,58] L. B. Guo,[37] R. P. Guo,[44] Y. P. Guo,[10,f] A. Guskov,[32,a] T. T. Han,[45] W. Y. Han,[35] X. Q. Hao,[18] F. A. Harris,[60] K. K. He,[50] K. L. He,[1,58] F. H. Heinsius,[4] C. H. Heinz,[31] Y. K. Heng,[1,53,58] C. Herold,[55] G. Y. Hou,[1,58] Y. R. Hou,[58] Z. L. Hou,[1] H. M. Hu,[1,58] J. F. Hu,[51,i] T. Hu,[1,53,58] Y. Hu,[1] G. S. Huang,[66,53] K. X. Huang,[54] L. Q. Huang,[28,58] X. T. Huang,[45] Y. P. Huang,[1] Z. Huang,[42,g] T. Hussain,[68] N. Hüsken,[25,31] W. Imoehl,[25] M. Irshad,[66,53] J. Jackson,[25] S. Jaeger,[4] S. Janchiv,[29] E. Jang,[50] J. H. Jeong,[50] Q. Ji,[1] Q. P. Ji,[18] X. B. Ji,[1,58] X. L. Ji,[1,53] Y. Y. Ji,[45] Z. K. Jia,[66,53] H. B. Jiang,[45] S. S. Jiang,[35] X. S. Jiang,[1,53,58] Y. Jiang,[58] J. B. Jiao,[45] Z. Jiao,[21] S. Jin,[38] Y. Jin,[61] M. Q. Jing,[1,58] T. Johansson,[70] N. Kalantar-Nayestanaki,[59] X. S. Kang,[36] R. Kappert,[59] M. Kavatsyuk,[59] B. C. Ke,[75] I. K. Keshk,[4] A. Khoukaz,[63] R. Kiuchi,[1] R. Kliemt,[12] L. Koch,[33] O. B. Kolcu,[57a] B. Kopf,[4] M. Kuemmel,[4] M. Kuessner,[4] A. Kupsc,[40,70] W. Kühn,[33] J. J. Lane,[62] J. S. Lange,[33] P. Larin,[17] A. Lavania,[24] L. Lavezzi,[69a,69c] Z. H. Lei,[66,53] H. Leithoff,[31] M. Lellmann,[31] T. Lenz,[31] C. Li,[39] C. Li,[43] C. H. Li,[35] Cheng Li,[66,53] D. M. Li,[75] F. Li,[1,53] G. Li,[1] H. Li,[47] H. Li,[66,53] H. B. Li,[1,58] H. J. Li,[18] H. N. Li,[51,i] J. Q. Li,[4] J. S. Li,[54] J. W. Li,[45] Ke Li,[1] L. J. Li,[1] L. K. Li,[1] Lei Li,[3] M. H. Li,[39] P. R. Li,[34,j,k] S. X. Li,[10] S. Y. Li,[56] T. Li,[45] W. D. Li,[1,58] W. G. Li,[1] X. H. Li,[66,53] X. L. Li,[45] Xiaoyu Li,[1,58] Y. G. Li,[42,g] Z. X. Li,[14] H. Liang,[66,53] H. Liang,[30] H. Liang,[1,58] Y. F. Liang,[49] Y. T. Liang,[28,58] G. R. Liao,[13] L. Z. Liao,[45] J. Libby,[24] A. Limphirat,[55] C. X. Lin,[54] D. X. Lin,[28,58] T. Lin,[1] B. J. Liu,[1] C. X. Liu,[1] D. Liu,[17,66] F. H. Liu,[48] Fang Liu,[1] Feng Liu,[6] G. M. Liu,[51,i] H. Liu,[34,j,k] H. B. Liu,[14] H. M. Liu,[1,58] Huanhuan Liu,[1] Huihui Liu,[19] J. B. Liu,[66,53] J. L. Liu,[67] J. Y. Liu,[1,58] K. Liu,[1] K. Y. Liu,[36] Ke Liu,[20] L. Liu,[66,53] Lu Liu,[39] M. H. Liu,[10,f] P. L. Liu,[1] Q. Liu,[58] S. B. Liu,[66,53] T. Liu,[10,f] W. K. Liu,[39] W. M. Liu,[66,53] X. Liu,[34,j,k] Y. Liu,[34,j,k] Y. B. Liu,[39] Z. A. Liu,[1,53,58] Z. Q. Liu,[45] X. C. Lou,[1,53,58] F. X. Lu,[54] H. J. Lu,[21] J. G. Lu,[1,53] X. L. Lu,[1] Y. Lu,[7] Y. P. Lu,[1,53] Z. H. Lu,[1] C. L. Luo,[37] M. X. Luo,[74] T. Luo,[10,f] X. L. Luo,[1,53] X. R. Lyu,[58] Y. F. Lyu,[39] F. C. Ma,[36] H. L. Ma,[1] L. L. Ma,[45] M. M. Ma,[1,58] Q. M. Ma,[1] R. Q. Ma,[1,58] R. T. Ma,[58] X. Y. Ma,[1,53] Y. Ma,[42,g] F. E. Maas,[17] M. Maggiora,[69a,69c] S. Maldaner,[4] S. Malde,[64] Q. A. Malik,[68] A. Mangoni,[26b] Y. J. Mao,[42,g] Z. P. Mao,[1] S. Marcello,[69a,69c] Z. X. Meng,[61] J. Messchendorp,[12,59] G. Mezzadri,[27a] H. Miao,[1] T. J. Min,[38] R. E. Mitchell,[25] X. H. Mo,[1,53,58] N. Yu. Muchnoi,[11,b] Y. Nefedov,[32] F. Nerling,[17,d] I. B. Nikolaev,[11,b] Z. Ning,[1,53] S. Nisar,[9,l] Y. Niu,[45] S. L. Olsen,[58] Q. Ouyang,[1,53,58] S. Pacetti,[26b,26c] X. Pan,[10,f] Y. Pan,[52] A. Pathak,[30] M. Pelizaeus,[4] H. P. Peng,[66,53] K. Peters,[12,d] J. L. Ping,[37] R. G. Ping,[1,58] S. Plura,[31] S. Pogodin,[32] V. Prasad,[66,53] F. Z. Qi,[1] H. Qi,[66,53] H. R. Qi,[56] M. Qi,[38] T. Y. Qi,[10,f] S. Qian,[1,53] W. B. Qian,[58] Z. Qian,[54] C. F. Qiao,[58] J. J. Qin,[67] L. Q. Qin,[13] X. P. Qin,[10,f] X. S. Qin,[45] Z. H. Qin,[1,53] J. F. Qiu,[1] S. Q. Qu,[56] K. H. Rashid,[68] C. F. Redmer,[31] K. J. Ren,[35] A. Rivetti,[69c] V. Rodin,[59] M. Rolo,[69c] G. Rong,[1,58] Ch. Rosner,[17] S. N. Ruan,[39] H. S. Sang,[66] A. Sarantsev,[32,c] Y. Schelhaas,[31] C. Schnier,[4] K. Schoenning,[70] M. Scodeggio,[27a,27b] K. Y. Shan,[10,f] W. Shan,[22] X. Y. Shan,[66,53] J. F. Shangguan,[50] L. G. Shao,[1,58] M. Shao,[66,53] C. P. Shen,[10,f] H. F. Shen,[1,58] X. Y. Shen,[1,58] B. A. Shi,[58] H. C. Shi,[66,53] J. Y. Shi,[1] Q. Q. Shi,[50] R. S. Shi,[1,58] X. Shi,[1,53] X. D. Shi,[66,53] J. J. Song,[18] W. M. Song,[30,1] Y. X. Song,[42,g] S. Sosio,[69a,69c] S. Spataro,[69a,69c] F. Stieler,[31] K. X. Su,[71] P. P. Su,[50] Y. J. Su,[58] G. X. Sun,[1] H. Sun,[58] H. K. Sun,[1] J. F. Sun,[18] L. Sun,[71] S. S. Sun,[1,58] T. Sun,[1,58] W. Y. Sun,[30] X. Sun,[23,h] Y. J. Sun,[66,53] Y. Z. Sun,[1] Z. T. Sun,[45] Y. H. Tan,[71] Y. X. Tan,[66,53] C. J. Tang,[49] G. Y. Tang,[1] J. Tang,[54] L. Y. Tao,[67] Q. T. Tao,[23,h] M. Tat,[64] J. X. Teng,[66,53] V. Thoren,[70] W. H. Tian,[47] Y. Tian,[28,58] I. Uman,[57b] B. Wang,[1] B. L. Wang,[58] C. W. Wang,[38] D. Y. Wang,[42,g] F. Wang,[67] H. J. Wang,[34,j,k] H. P. Wang,[1,58] K. Wang,[1,53] L. L. Wang,[1] M. Wang,[45] M. Z. Wang,[42,g] Meng Wang,[1,58] S. Wang,[13] S. Wang,[10,f] T. Wang,[10,f] T. J. Wang,[39] W. Wang,[54] W. H. Wang,[71] W. P. Wang,[66,53] X. Wang,[42,g] X. F. Wang,[34,j,k] X. L. Wang,[10,f] Y. Wang,[56] Y. D. Wang,[41] Y. F. Wang,[1,53,58] Y. H. Wang,[43] Y. Q. Wang,[1] Yaqian Wang,[16,1] Z. Wang,[1,53] Z. Y. Wang,[1,58] Ziyi Wang,[58] D. H. Wei,[13] F. Weidner,[63] S. P. Wen,[1] D. J. White,[62] U. Wiedner,[4] G. Wilkinson,[64] M. Wolke,[70] L. Wollenberg,[4] J. F. Wu,[1,58] L. H. Wu,[1] L. J. Wu,[1,58] X. Wu,[10,f]

X. H. Wu,[30] Y. Wu,[66] Y. J. Wu,[28] Z. Wu,[1,53] L. Xia,[66,53] T. Xiang,[42,g] D. Xiao,[34,j,k] G. Y. Xiao,[38] H. Xiao,[10,f] S. Y. Xiao,[1] Y. L. Xiao,[10,f] Z. J. Xiao,[37] C. Xie,[38] X. H. Xie,[42,g] Y. Xie,[45] Y. G. Xie,[1,53] Y. H. Xie,[6] Z. P. Xie,[66,53] T. Y. Xing,[1,58] C. F. Xu,[1] C. J. Xu,[54] G. F. Xu,[1] H. Y. Xu,[61] Q. J. Xu,[15] X. P. Xu,[50] Y. C. Xu,[58] Z. P. Xu,[38] F. Yan,[10,f] L. Yan,[10,f] W. B. Yan,[66,53] W. C. Yan,[75] H. J. Yang,[46,e] H. L. Yang,[30] H. X. Yang,[1] L. Yang,[47] S. L. Yang,[58] Tao Yang,[1] Y. F. Yang,[39] Y. X. Yang,[1,58] Yifan Yang,[1,58] M. Ye,[1,53] M. H. Ye,[8] J. H. Yin,[1] Z. Y. You,[54] B. X. Yu,[1,53,58] C. X. Yu,[39] G. Yu,[1,58] T. Yu,[67] X. D. Yu,[42,g] C. Z. Yuan,[1,58] L. Yuan,[2] S. C. Yuan,[1] X. Q. Yuan,[1] Y. Yuan,[1,58] Z. Y. Yuan,[54] C. X. Yue,[35] A. A. Zafar,[68] F. R. Zeng,[45] X. Zeng,[6] Y. Zeng,[23,h] Y. H. Zhan,[54] A. Q. Zhang,[1] B. L. Zhang,[1] B. X. Zhang,[1] D. H. Zhang,[39] G. Y. Zhang,[18] H. Zhang,[66] H. H. Zhang,[30] H. H. Zhang,[54] H. Y. Zhang,[1,53] J. L. Zhang,[72] J. Q. Zhang,[37] J. W. Zhang,[1,53,58] J. X. Zhang,[34,j,k] J. Y. Zhang,[1] J. Z. Zhang,[1,58] Jianyu Zhang,[1,58] Jiawei Zhang,[1,58] L. M. Zhang,[56] L. Q. Zhang,[54] Lei Zhang,[38] P. Zhang,[1] Q. Y. Zhang,[35,75] Shuihan Zhang,[1,58] Shulei Zhang,[23,h] X. D. Zhang,[41] X. M. Zhang,[1] X. Y. Zhang,[45] X. Y. Zhang,[50] Y. Zhang,[64] Y. T. Zhang,[75] Y. H. Zhang,[1,53] Yan Zhang,[66,53] Yao Zhang,[1] Z. H. Zhang,[1] Z. Y. Zhang,[39] Z. Y. Zhang,[71] G. Zhao,[1] J. Zhao,[35] J. Y. Zhao,[1,58] J. Z. Zhao,[1,53] Lei Zhao,[66,53] Ling Zhao,[1] M. G. Zhao,[39] S. J. Zhao,[75] Y. B. Zhao,[1,53] Y. X. Zhao,[28,58] Z. G. Zhao,[66,53] A. Zhemchugov,[32,a] B. Zheng,[67] J. P. Zheng,[1,53] Y. H. Zheng,[58] B. Zhong,[37] C. Zhong,[67] X. Zhong,[54] H. Zhou,[45] L. P. Zhou,[1,58] X. Zhou,[71] X. K. Zhou,[58] X. R. Zhou,[66,53] X. Y. Zhou,[35] Y. Z. Zhou,[10,f] J. Zhu,[39] K. Zhu,[1] K. J. Zhu,[1,53,58] L. X. Zhu,[58] S. H. Zhu,[65] S. Q. Zhu,[38] T. J. Zhu,[72] W. J. Zhu,[10,f] Y. C. Zhu,[66,53] Z. A. Zhu,[1,58] and J. H. Zou[1]

(BESIII Collaboration)

[1]*Institute of High Energy Physics, Beijing 100049, People's Republic of China*
[2]*Beihang University, Beijing 100191, People's Republic of China*
[3]*Beijing Institute of Petrochemical Technology, Beijing 102617, People's Republic of China*
[4]*Bochum Ruhr-University, D-44780 Bochum, Germany*
[5]*Carnegie Mellon University, Pittsburgh, Pennsylvania 15213, USA*
[6]*Central China Normal University, Wuhan 430079, People's Republic of China*
[7]*Central South University, Changsha 410083, People's Republic of China*
[8]*China Center of Advanced Science and Technology, Beijing 100190, People's Republic of China*
[9]*COMSATS University Islamabad, Lahore Campus, Defence Road, Off Raiwind Road, 54000 Lahore, Pakistan*
[10]*Fudan University, Shanghai 200433, People's Republic of China*
[11]*G.I. Budker Institute of Nuclear Physics SB RAS (BINP), Novosibirsk 630090, Russia*
[12]*GSI Helmholtzcentre for Heavy Ion Research GmbH, D-64291 Darmstadt, Germany*
[13]*Guangxi Normal University, Guilin 541004, People's Republic of China*
[14]*Guangxi University, Nanning 530004, People's Republic of China*
[15]*Hangzhou Normal University, Hangzhou 310036, People's Republic of China*
[16]*Hebei University, Baoding 071002, People's Republic of China*
[17]*Helmholtz Institute Mainz, Staudinger Weg 18, D-55099 Mainz, Germany*
[18]*Henan Normal University, Xinxiang 453007, People's Republic of China*
[19]*Henan University of Science and Technology, Luoyang 471003, People's Republic of China*
[20]*Henan University of Technology, Zhengzhou 450001, People's Republic of China*
[21]*Huangshan College, Huangshan 245000, People's Republic of China*
[22]*Hunan Normal University, Changsha 410081, People's Republic of China*
[23]*Hunan University, Changsha 410082, People's Republic of China*
[24]*Indian Institute of Technology Madras, Chennai 600036, India*
[25]*Indiana University, Bloomington, Indiana 47405, USA*
[26a]*INFN Laboratori Nazionali di Frascati, I-00044, Frascati, Italy*
[26b]*INFN Sezione di Perugia, I-06100, Perugia, Italy*
[26c]*University of Perugia, I-06100, Perugia, Italy*
[27a]*INFN Sezione di Ferrara, I-44122, Ferrara, Italy*
[27b]*University of Ferrara, I-44122, Ferrara, Italy*
[28]*Institute of Modern Physics, Lanzhou 730000, People's Republic of China*
[29]*Institute of Physics and Technology, Peace Avenue 54B, Ulaanbaatar 13330, Mongolia*
[30]*Jilin University, Changchun 130012, People's Republic of China*
[31]*Johannes Gutenberg University of Mainz, Johann-Joachim-Becher-Weg 45, D-55099 Mainz, Germany*
[32]*Joint Institute for Nuclear Research, 141980 Dubna, Moscow region, Russia*
[33]*Justus-Liebig-Universitaet Giessen, II. Physikalisches Institut, Heinrich-Buff-Ring 16, D-35392 Giessen, Germany*
[34]*Lanzhou University, Lanzhou 730000, People's Republic of China*

[35]Liaoning Normal University, Dalian 116029, People's Republic of China
[36]Liaoning University, Shenyang 110036, People's Republic of China
[37]Nanjing Normal University, Nanjing 210023, People's Republic of China
[38]Nanjing University, Nanjing 210093, People's Republic of China
[39]Nankai University, Tianjin 300071, People's Republic of China
[40]National Centre for Nuclear Research, Warsaw 02-093, Poland
[41]North China Electric Power University, Beijing 102206, People's Republic of China
[42]Peking University, Beijing 100871, People's Republic of China
[43]Qufu Normal University, Qufu 273165, People's Republic of China
[44]Shandong Normal University, Jinan 250014, People's Republic of China
[45]Shandong University, Jinan 250100, People's Republic of China
[46]Shanghai Jiao Tong University, Shanghai 200240, People's Republic of China
[47]Shanxi Normal University, Linfen 041004, People's Republic of China
[48]Shanxi University, Taiyuan 030006, People's Republic of China
[49]Sichuan University, Chengdu 610064, People's Republic of China
[50]Soochow University, Suzhou 215006, People's Republic of China
[51]South China Normal University, Guangzhou 510006, People's Republic of China
[52]Southeast University, Nanjing 211100, People's Republic of China
[53]State Key Laboratory of Particle Detection and Electronics, Beijing 100049, Hefei 230026, People's Republic of China
[54]Sun Yat-Sen University, Guangzhou 510275, People's Republic of China
[55]Suranaree University of Technology, University Avenue 111, Nakhon Ratchasima 30000, Thailand
[56]Tsinghua University, Beijing 100084, People's Republic of China
[57a]Turkish Accelerator Center Particle Factory Group, Istinye University, 34010, Istanbul, Turkey
[57b]Near East University, Nicosia, North Cyprus, Mersin 10, Turkey
[58]University of Chinese Academy of Sciences, Beijing 100049, People's Republic of China
[59]University of Groningen, NL-9747 AA Groningen, The Netherlands
[60]University of Hawaii, Honolulu, Hawaii 96822, USA
[61]University of Jinan, Jinan 250022, People's Republic of China
[62]University of Manchester, Oxford Road, Manchester, M13 9PL, United Kingdom
[63]University of Muenster, Wilhelm-Klemm-Strasse 9, 48149 Muenster, Germany
[64]University of Oxford, Keble Road, Oxford OX13RH, United Kingdom
[65]University of Science and Technology Liaoning, Anshan 114051, People's Republic of China
[66]University of Science and Technology of China, Hefei 230026, People's Republic of China
[67]University of South China, Hengyang 421001, People's Republic of China
[68]University of the Punjab, Lahore-54590, Pakistan
[69a]University of Turin and INFN, University of Turin, I-10125, Turin, Italy
[69b]University of Eastern Piedmont, I-15121, Alessandria, Italy
[69c]INFN, I-10125, Turin, Italy
[70]Uppsala University, Box 516, SE-75120 Uppsala, Sweden
[71]Wuhan University, Wuhan 430072, People's Republic of China
[72]Xinyang Normal University, Xinyang 464000, People's Republic of China
[73]Yunnan University, Kunming 650500, People's Republic of China
[74]Zhejiang University, Hangzhou 310027, People's Republic of China
[75]Zhengzhou University, Zhengzhou 450001, People's Republic of China

[a]Also at the Moscow Institute of Physics and Technology, Moscow 141700, Russia.
[b]Also at the Novosibirsk State University, Novosibirsk, 630090, Russia.
[c]Also at the NRC "Kurchatov Institute," PNPI, 188300, Gatchina, Russia.
[d]Also at Goethe University Frankfurt, 60323 Frankfurt am Main, Germany.
[e]Also at Key Laboratory for Particle Physics, Astrophysics and Cosmology, Ministry of Education; Shanghai Key Laboratory for Particle Physics and Cosmology; Institute of Nuclear and Particle Physics, Shanghai 200240, People's Republic of China.
[f]Also at Key Laboratory of Nuclear Physics and Ion-beam Application (MOE) and Institute of Modern Physics, Fudan University, Shanghai 200443, People's Republic of China.
[g]Also at State Key Laboratory of Nuclear Physics and Technology, Peking University, Beijing 100871, People's Republic of China.
[h]Also at School of Physics and Electronics, Hunan University, Changsha 410082, China.
[i]Also at Guangdong Provincial Key Laboratory of Nuclear Science, Institute of Quantum Matter, South China Normal University, Guangzhou 510006, China.
[j]Also at Frontiers Science Center for Rare Isotopes, Lanzhou University, Lanzhou 730000, People's Republic of China.
[k]Also at Lanzhou Center for Theoretical Physics, Lanzhou University, Lanzhou 730000, People's Republic of China.
[l]Also at the Department of Mathematical Sciences, IBA, Karachi, Pakistan.

(Received 19 October 2022; accepted 19 July 2023; published 3 August 2023)

Based on e^+e^- collision data corresponding to an integrated luminosity of 4.5 fb^{-1} collected at the center-of-mass energies between 4.600 and 4.699 GeV with the BESIII detector at BEPCII, the absolute branching fraction of the inclusive decay $\bar{\Lambda}_c^- \to \bar{n} + X$, where X refers to any possible final state particles, is measured. The absolute branching fraction is determined to be $\mathcal{B}(\bar{\Lambda}_c^- \to \bar{n} + X) = (32.4 \pm 0.7 \pm 1.5)\%$, where the first uncertainty is statistical and the second systematic. Assuming CP symmetry, the measurement indicates that about one fourth of Λ_c^+ ($\bar{\Lambda}_c^-$) decay modes with a neutron (an antineutron) in the final state have not been observed.

DOI: 10.1103/PhysRevD.108.L031101

The Λ_c^+ is the lightest charmed baryon, and the measurement of the properties of Λ_c^+ provides key input for studying heavier charmed baryons [1] and bottom baryons [2,3], as well as understanding the dynamics of light quarks in the environment with a heavy quark [4]. However, there is no reliable phenomenological model calculation describing the complicated physics of charmed baryon decays. Therefore, comprehensive and precise experimental studies of the Λ_c^+ decays are highly desirable.

Experimentally, since the discovery of the Λ_c^+ baryon in 1979 [5], which eventually decays to a proton or a neutron, its decays with a proton in the final state have been studied extensively. However, information about decays with a neutron in the final state is sparse. Recently, the BESIII Collaboration measured the absolute branching fraction of decay $\Lambda_c^+ \to n\pi^+$ to be $(6.6 \pm 1.2 \pm 0.4) \times 10^{-4}$ [6], where the double-tag (DT) approach [7] is used, and the neutrons are treated as missing particles and inferred under the laws of conservation of energy and momentum. This is the first-time measurement of the singly Cabibbo suppressed mode involving a neutron directly in the final state in the Λ_c^+ decays. Up to now, there are still very few measurements that directly observed neutron signals in the Λ_c^+ decays [6,8,9], including the decays $\Lambda_c^+ \to \Sigma^- 2\pi^+$ and $\Sigma^-\pi^0 2\pi^+$ [10] where the Σ^- is reconstructed with its dominant decay mode $\Sigma^- \to n\pi^-$. All the measurements implicitly include charge-conjugate modes. Combing all the known exclusive decays of Λ_c^+ summarized by the Particle Data Group (PDG) [11], the total branching fraction of the decays with a proton or a neutron in the final state is about 44% or 25%, respectively, which include both the direct decay channels of Λ_c^+ and the decays from intermediate particles, i.e. Λ, Σ, and Ξ. There are still lots of unknown decay channels of Λ_c^+ baryon to be explored experimentally.

The inclusive decay $\Lambda_c^+ \to n + X$, where X refers to any possible particle system, has not yet been studied experimentally, due to the difficulty in discriminating neutron signals from neutral noises. In 1992, Ref. [13] estimated the inclusive branching fractions of both $\Lambda_c^+ \to p + X$ and $\Lambda_c^+ \to n + X$ to be $(50 \pm 16)\%$, inferred from the known exclusive B-meson decays and the fact that all Λ_c^+ must decay to either proton or neutron. High precision measurements on the inclusive decays of Λ_c^+ are crucial to point out the direction of searches for unknown channels. Furthermore, the results of inclusive decays will provide direct information about whether there exists a significant difference between the decays of Λ_c^+ with a proton and a neutron in the final state. The investigation of the isospin symmetry between them is important input to theoretical estimation of the lifetime of the charmed baryon Λ_c^+.

Compared with the neutron, an antineutron has larger energy deposition in an electromagnetic calorimeter (EMC) due to its annihilation reaction with materials, which allows for good discrimination against the contamination from the electromagnetic showers of photon. Hence, our measurement is conducted with the antiparticle decay $\bar{\Lambda}_c^- \to \bar{n} + X$, which is supposed to yield the same result as the $\Lambda_c^+ \to n + X$ if the CP violation effect is ignored.

In this paper, taking advantage of the excellent BESIII detector performance and of the $\Lambda_c^+\bar{\Lambda}_c^-$ production just above the mass threshold, the first measurement of absolute branching fraction of the $\bar{\Lambda}_c^- \to \bar{n} + X$ decay is reported using e^+e^- collision data collected with the BESIII detector at seven center-of-mass (c.m.) energies between 4.600 and 4.699 GeV, corresponding to an integrated luminosity of 4.5 fb^{-1}. The integrated luminosities at these c.m. energies [14,15] are summarized in Table I.

A detailed description of the design and performance of the BESIII detector can be found in Ref. [16]. Simulated samples are produced with a GEANT4-based [17] Monte Carlo (MC) toolkit, which includes the geometric description of the BESIII detector. The signal MC samples of $e^+e^- \to \Lambda_c^+\bar{\Lambda}_c^-$, with Λ_c^+ decaying into the specific tag mode $\Lambda_c^+ \to pK^-\pi^+$ and $\bar{\Lambda}_c^-$ going to any possible processes containing the already measured [6,8–11] and

TABLE I. The integrated luminosity ($\mathcal{L}_{\rm int}$), ST yields, and the detection efficiencies of the ST and DT selections for the data samples at seven c.m. energies. The uncertainties are statistical only.

$\sqrt{s}$ (GeV)	$\mathcal{L}_{\rm int}$ (pb^{-1})	$N_i^{\rm ST}$	$\epsilon_i^{\rm ST}$ (%)	$\epsilon_i^{\rm DT}$ (%)
4.600	586.9 ± 0.1	3266 ± 62	51.0 ± 0.2	19.1 ± 0.1
4.612	103.8 ± 0.1	587 ± 28	50.2 ± 0.2	19.2 ± 0.1
4.628	521.5 ± 0.1	2967 ± 64	49.5 ± 0.2	19.1 ± 0.1
4.641	552.4 ± 0.1	3201 ± 66	49.0 ± 0.2	18.9 ± 0.1
4.661	529.6 ± 0.1	3080 ± 63	48.0 ± 0.2	18.5 ± 0.1
4.682	1669.3 ± 0.2	8863 ± 107	47.3 ± 0.2	18.2 ± 0.1
4.699	536.5 ± 0.1	2613 ± 59	46.4 ± 0.2	17.8 ± 0.1

predicted [12] ones with an $\bar{n}$ in the final state, are used to determine the detection efficiencies. They are generated for each individual c.m. energy with the generator KKMC [18] by incorporating initial-state radiation (ISR) effects and the beam energy spread. The $\bar{n}$ candidates include the ones both from the interaction point (IP) and from intermediate particles, i.e. Λ, Σ and Ξ. The inclusive MC samples, which consist of $\Lambda_c^+\bar{\Lambda}_c^-$, charmed meson $D_{(s)}^{(*)}$ pair production, ISR return to the charmonium(-like) ψ states at lower masses, and continuum processes $e^+e^- \to q\bar{q}$ ($q = u, d, s$), are generated to survey potential backgrounds. Particle decays are modeled with EVTGEN [19,20] using branching fractions taken from the PDG [11], when available, or otherwise estimated with LUNDCHARM [21,22]. Final state radiation from charged final state particles is incorporated using PHOTOS [23].

The DT approach [7] is implemented to measure the absolute branching fraction of $\bar{\Lambda}_c^- \to \bar{n} + X$. Taking advantage of a large branching fraction and a high signal-to-background ratio, Λ_c^+ baryons are reconstructed in the $\Lambda_c^+ \to pK^-\pi^+$ decay mode, and are referred to as the single-tag (ST) candidates. Events in which the signal decay $\bar{\Lambda}_c^- \to \bar{n} + X$ is reconstructed in the system recoiling against the Λ_c^+ candidates of the ST sample are denoted as the DT candidates.

Charged tracks detected in the helium-based multilayer drift chamber (MDC) are required to be within a polar angle (θ) range of $|\cos\theta| < 0.93$, where θ is defined with respect to the z axis, which is the symmetry axis of the MDC. Their distances of the closest approach to the IP must be less than 10 cm along the z axis, and less than 1 cm in the transverse plane. The particle identification is implemented by combining measurements of the ionization energy loss (dE/dx) in the MDC and the flight time in the time-of-flight system, and to each charged track a particle type of pion, kaon, or proton is assigned, according to which assignment has the highest probability.

The ST Λ_c^+ candidates are identified using the beam constrained mass $M_{\rm BC} = \sqrt{E_{\rm beam}^2/c^4 - |\vec{p}_{\Lambda_c^+}|^2/c^2}$ and energy difference $\Delta E = E_{\Lambda_c^+} - E_{\rm beam}$, where $E_{\rm beam}$ is the beam energy, and $E_{\Lambda_c^+}$ ($\vec{p}_{\Lambda_c^+}$) is the energy (momentum) of the Λ_c^+ candidates in the c.m. frame. The Λ_c^+ candidates are required to satisfy the requirement $\Delta E \in (-34, 20)$ MeV. The asymmetric interval takes into account the effects of ISR and corresponds to 3 times the resolution around the peak. If there is more than one $pK^-\pi^+$ combination satisfying the above requirements, the one with the minimum $|\Delta E|$ is kept.

The $M_{\rm BC}$ distributions of candidate events for the ST mode with data samples at different c.m. energies are illustrated in Fig. 1, where clear Λ_c^+ signals are observed. No peaking backgrounds are found with the investigation of the inclusive MC samples. To obtain the ST yields,

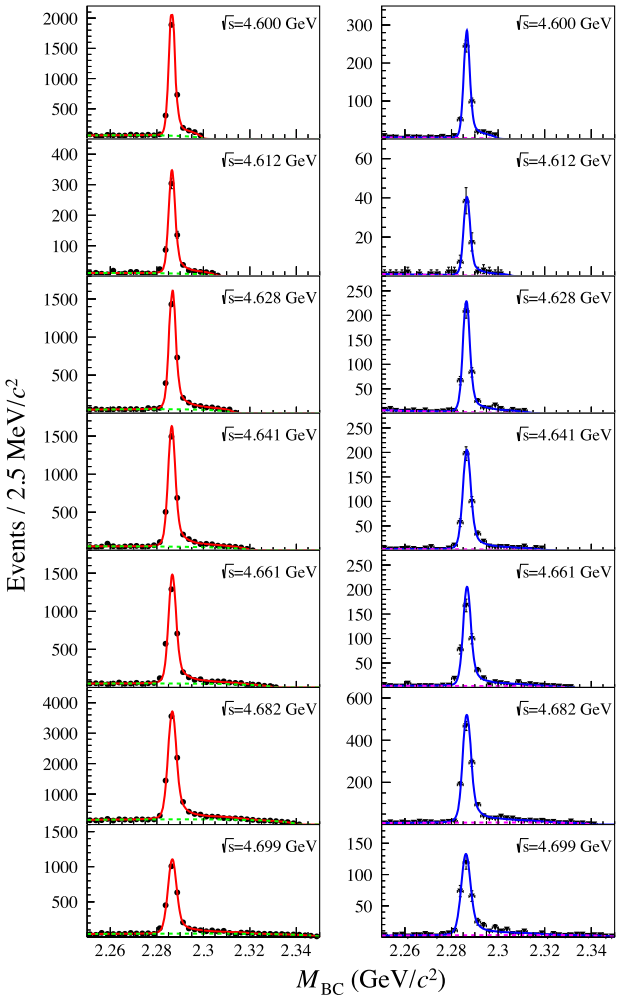

FIG. 1. The $M_{\rm BC}$ distributions of Λ_c^+ at seven c.m. energies, and the data distributions are described by points (left column) or triangles (right column) with error bars. The seven figures on the left column represent the results after the ST selections, and those on the right are obtained with both ST and $\bar{n}$ selections. The (red) solid curves indicate the fit results, and the (green) dashed curves describe the background shapes after the ST selections. The (blue) solid curves indicate the fit results, and the (pink) dashed curves describe the background shapes after applying the $\bar{n}$ selections.

unbinned maximum likelihood fits on these $M_{\rm BC}$ distributions are performed, where the signal is modeled with the MC-simulated distribution convolved with a Gaussian function taking into account the resolution difference between data and MC simulation, and the background distribution is described by an ARGUS function [24] with the truncation parameter fixed to the corresponding $E_{\rm beam}$. The candidates within $M_{\rm BC} \in (2.275, 2.31)$ GeV/c^2 are retained for further analysis, and the signal yields for the data samples at different c.m. energies are summarized in Table I. The sum of ST yields for all data samples is $24,577 \pm 179$, where the uncertainty is statistical.

The decay $\bar{\Lambda}_c^- \to \bar{n} + X$ is searched for among the remaining tracks and showers recoiling against the ST Λ_c^+ candidates. Neutral showers are identified in the EMC. The deposited energy of each shower must be more than 25 MeV in the barrel region ($|\cos\theta| < 0.8$) and more than 50 MeV in the end cap region ($0.86 < |\cos\theta| < 0.92$). To suppress electronic noise and showers unrelated to the event, the difference between the EMC time and the event start time is required to be within [0, 700] ns. The most energetic shower is taken as the $\bar{n}$ candidate. The angle between the charged track and shower is required to be greater than 20 degrees. To discriminate the $\bar{n}$ shower from showers caused by photons and neutrons, three variables are used for further selection: the deposited energy ($E_{\bar{n}}$) in the EMC, the second moment of shower shape ($S_{\bar{n}} = \Sigma_i E_i r_i^2 / \Sigma_i E_i$, where E_i is the energy deposited in the ith crystal of the shower and r_i is the distance from the center of that crystal to the center of the shower), and the number of hit crystals ($H_{\bar{n}}$) for the primary shower. The most energetic shower is required to have $E_{\bar{n}} > 0.48$ GeV, $H_{\bar{n}} > 20$, and $S_{\bar{n}} > 18$ cm^2. To suppress contamination from the decays with a $\bar{p}$ particle in the final state, the candidate events are further required to be without any tracks identified as $\bar{p}$ and having a distance of closest approach to the IP within 20 cm along the z axis.

In contrast to photons and electrons, the interaction of $\bar{n}$ with materials is very difficult to model, and there exists more than 10% deviation in detection efficiency between data and MC simulation for the $\bar{n}$ induced clusters in the EMC. To solve this issue, a model-independent data-driven method [25] has been developed to simulate the detector response of the $\bar{n}$ at BESIII. The detector response in data is investigated with a control sample of 16.2 million $\bar{n}$ candidates selected in the process $J/\psi \to p\bar{n}\pi^-$ at $\sqrt{s} =$ 3.097 GeV [26]. Firstly, the efficiency of the requirements $E_{\bar{n}} > 0.48$ GeV, $H_{\bar{n}} > 20$, and $S_{\bar{n}} > 18$ cm^2 is derived in different finite bins ($\varepsilon_{\rm bin}$) of the two-dimensional distribution of the momentum and polar angle $\cos\theta_{\bar{n}}$ of $\bar{n}$ by comparing the yields of the $\bar{n}$ candidates in the control sample with and without imposing the above requirements. In the signal MC samples of the process $\bar{\Lambda}_c^- \to \bar{n} + X$, each accepted event with these requirements is determined, if a random number, uniformly generated between 0 and 1, and is less than the value of $\varepsilon_{\rm bin}$ in the bin that the event belongs to. Then, the efficiency of the $\bar{n}$ selections is calculated by comparing the number of accepted events, summed over all bins, with the total number of events at the generator level. Secondly, the probability density function and the cumulative distribution function (CDF) of the deposited energy $E_{\bar{n}}$, after applying the selection criteria, are evaluated in these different bins of momentum and $\cos\theta_{\bar{n}}$ with the control sample. Then, the value of $E_{\bar{n}}$ for each accepted event, in the signal MC samples, is sampled based on the CDF of $E_{\bar{n}}$ in the bin that the event belongs to. After imposing all the selections mentioned above, the distribution of $E_{\bar{n}}$ for the accepted DT candidates from the combined data samples at seven c.m. energies is shown in Fig. 2, where the data-driven method has been applied in the prediction of signal process $\bar{\Lambda}_c^- \to \bar{n} + X$ and the simulated shape describes the data well.

The potential backgrounds can be classified into two categories: those directly originated from continuum hadron

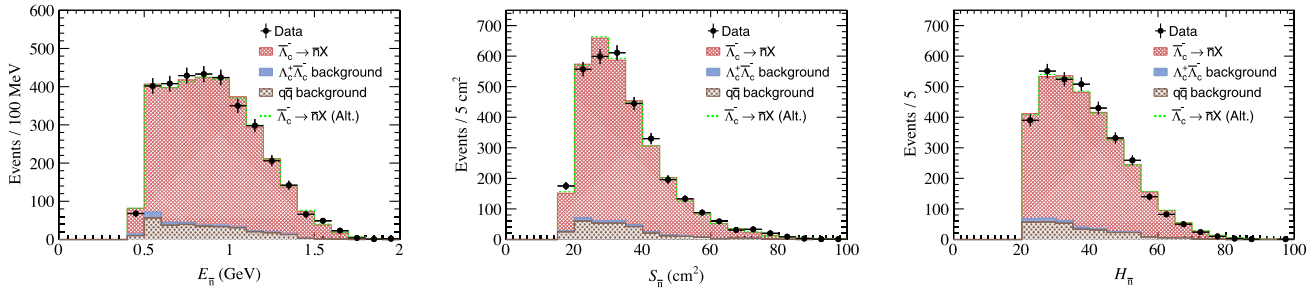

FIG. 2. The stacked distribution of $E_{\bar{n}}$ (a), $S_{\bar{n}}$ (b) and $H_{\bar{n}}$ (c) for the accepted DT candidates in the region $M_{\rm BC} \in (2.275, 2.31)$ GeV/c^2 from the combined seven data samples. The black points with error bars are data. The red shaded histogram is the signal that is obtained with the data-driven method, and the green one describes the alternative signal shape obtained with a Monte Carlo sample with only the observed decay modes. The blue and brown shaded histograms are the two background components, where the $\Lambda_c^+\bar{\Lambda}_c^-$ is modeled with the inclusive MC sample of $\Lambda_c^+ \to p + X$ and the $q\bar{q}$ is estimated with events in the sideband region of $M_{\rm BC} \in (2.20, 2.26)$ GeV/c^2 and normalized to the region $M_{\rm BC} \in (2.275, 2.31)$ GeV/c^2.

production in the e^+e^- annihilation (denoted as $q\bar{q}$ background hereafter) and those from the $e^+e^- \to \Lambda_c^+\bar{\Lambda}_c^-$ events (denoted as $\Lambda_c^+\bar{\Lambda}_c^-$ background hereafter) except for the signal of $\bar{\Lambda}_c^- \to \bar{n} + X$. The resultant $E_{\bar{n}}$ distribution is depicted in Fig. 2, where the events are selected in the region $M_{\rm BC} \in (2.275, 2.31)$ GeV/c^2. In Fig. 2, the $q\bar{q}$ contamination, which is the major background component, is estimated with events in the sideband region $M_{\rm BC} \in (2.20, 2.26)$ GeV/c^2 and normalized to the region $M_{\rm BC} \in (2.275, 2.31)$ GeV/c^2. The normalization factor is calculated with the event numbers in these two regions which are determined by integrating the ARGUS functions in the fitting to the ST $M_{\rm BC}$ distributions. The $\Lambda_c^+\bar{\Lambda}_c^-$ background is modeled with the inclusive MC sample of $\bar{\Lambda}_c^- \to \bar{p} + X$.

The yield of signal $\bar{\Lambda}_c^- \to \bar{n} + X$ is obtained by performing unbinned maximum-likelihood fits on the $M_{\rm BC}$ distributions of ST Λ_c^+ after applying the $\bar{n}$ selections. The procedure is similar to the one used to obtain the ST yields. The fitting curves for data samples at different c.m. energies are illustrated in Fig. 1, and the signal yields are obtained within $M_{\rm BC} \in (2.275, 2.31)$ GeV/c^2. The $\Lambda_c^+\bar{\Lambda}_c^-$ contamination has the same shape as the signal process due to the undetected $\bar{p}$ tracks and misidentified $\bar{n}$ showers, and it is estimated with the inclusive MC samples and subtracted from observed signal yields. The fitting results and $\Lambda_c^+\bar{\Lambda}_c^-$ background are summarized in Table II.

The branching fraction ($\mathcal{B}$) of decay $\bar{\Lambda}_c^- \to \bar{n} + X$ is determined as

$$\mathcal{B} = \frac{N_{\rm sig}^{\rm DT} - N_{\rm bkg-mc}^{\Lambda_c^+\bar{\Lambda}_c^-}}{\sum_i N_i^{\rm ST} \cdot (\epsilon_i^{\rm DT}/\epsilon_i^{\rm ST})},$$

where $N_{\rm sig}^{\rm DT}$ is the signal yield from the unbinned maximum-likelihood fit, and $N_{\rm bkg-mc}^{\Lambda_c^+\bar{\Lambda}_c^-}$ is the estimated $\Lambda_c^+\bar{\Lambda}_c^-$ background from the inclusive MC samples. The subscript i represents the data samples at different c.m. energies. The parameters $N_i^{\rm ST}$, $\epsilon_i^{\rm ST}$ and $\epsilon_i^{\rm DT}$ are the ST yields, ST and DT efficiencies, respectively. The ST and DT efficiencies are summarized in Table I, where the efficiency of $\bar{n}$ selections is already corrected with the data-driven method [25]. The branching fraction is determined to be $\mathcal{B}(\bar{\Lambda}_c^- \to \bar{n} + X) = (32.4 \pm 0.7 \pm 1.5)\%$, where the first uncertainty is statistical and the second systematic.

TABLE II. Yields of the fitting results and the corresponding background estimation for the data samples at different c.m. energies. The uncertainty is statistical only.

$\sqrt{s}$ (GeV)	$N_{\rm sig}^{\rm fit}$	$N_{\rm bkg-mc}^{\Lambda_c^+\bar{\Lambda}_c^-}$
4.600	408 ± 23	4.4 ± 0.3
4.612	66 ± 9	1.4 ± 0.2
4.628	395 ± 23	6.7 ± 0.4
4.641	405 ± 23	6.9 ± 0.5
4.661	392 ± 22	7.1 ± 0.4
4.682	1135 ± 36	20.5 ± 0.6
4.699	304 ± 19	5.8 ± 0.4
Sum	3105 ± 62	52.9 ± 1.1

The systematic uncertainties for the branching fraction measurement include those associated with the ST yields, detection efficiencies of the ST Λ_c^+ and the DT selections. As the DT technique is adopted, the systematic uncertainties associated with the ST detection efficiency cancel out.

The uncertainty in the ST yields is 0.5%, which arises from the statistical uncertainty and a systematic component coming from the fit to the $M_{\rm BC}$ distribution. The uncertainty is evaluated by floating the truncation parameter of the ARGUS function and changing the single Gaussian function to a double Gaussian function. The uncertainty associated with the finite size of the signal MC samples is 0.3%. The uncertainty arising from the signal modeling is 4.1%, which combines two sources. The first is due to unknown processes in the MC production, which is investigated by generating alternative signal MC samples only with the known $\bar{n}$ processes in the PDG [11]. The second one is the imperfect simulation of the $E_{\bar{n}}$ distribution, which is estimated by comparing the difference in the detection efficiencies between the results with and without reweighting the MC-simulated $E_{\bar{n}}$ distribution to data, where all the signal selection criteria in the analysis are applied except for the $E_{\bar{n}}$ requirement. For each case, the change of the signal efficiencies is taken as the systematic uncertainty. The uncertainty in the fit strategy of extracting the signal yields is assigned to be 0.4%, which is estimated by floating the truncation parameter of the ARGUS function and changing the single Gaussian function to a double Gaussian function. The uncertainty arising from $\Lambda_c^+\bar{\Lambda}_c^-$ background estimation is studied by generating alternative inclusive MC samples only with the known processes in the PDG [11], and comparing the background yields between the nominal and alternative MC samples. The difference of signal yields after subtracting the estimated $\Lambda_c^+\bar{\Lambda}_c^-$ background, 1.0%, is assigned as the corresponding uncertainty. The uncertainty due to $\bar{n}$ selections is assigned to be 2.0%, as explained in Ref. [25]. All other uncertainties are negligible. Assuming that all the systematic uncertainties are uncorrelated, the total uncertainty is then taken to be the quadratic sum of the individual values, which is 4.7%.

In summary, the first measurement of the absolute branching fraction of the inclusive decay $\bar{\Lambda}_c^- \to \bar{n} + X$ is reported using 4.5 fb^{-1} e^+e^- collision data collected at seven c.m. energies between 4.600 and 4.699 GeV with the BESIII detector. The absolute branching fraction is determined to be $\mathcal{B}(\bar{\Lambda}_c^- \to \bar{n} + X) = (32.4 \pm 0.7 \pm 1.5)\%$, where the first uncertainty is statistical and the second systematic. Neglecting the effect of CP violation, the inclusive decay $\Lambda_c^+ \to n + X$ should have the same value as $\bar{\Lambda}_c^- \to \bar{n} + X$. The measurement significantly improves the precision up to 5%, compared with the previous result

of this inclusive decay, $(50 \pm 16)\%$, inferred from the B-meson decays [13]. The branching fraction of sum over all the known exclusive decays with a neutron in the final state is about $(25.4 \pm 0.8)\%$ [6,9,11], where the uncertainties of all the modes are treated without correlation. It means that about one fourth of the Λ_c^+ decays with a neutron in the final state remain to be explored in experiments.

ACKNOWLEDGMENTS

The BESIII Collaboration thanks the staff of BEPCII and the IHEP computing center and the supercomputing center of the University of Science and Technology of China (USTC) for their strong support. This work is supported in part by the National Key R&D Program of China under Contracts No. 2020YFA0406400, No. 2020YFA0406300; National Natural Science Foundation of China (NSFC) under Contracts No. 11635010, No. 11735014, No. 11835012, No. 11935015, No. 11935016, No. 11935018, No. 11961141012, No. 12022510, No. 12025502, No. 12035009, No. 12035013, No. 12192260, No. 12192261, No. 12192262, No. 12192263, No. 12192264, No. 12192265, No. 12005311; the Fundamental Research Funds for the Central Universities, Sun Yat-sen University, University of Science and Technology of China; 100 Talents Program of Sun Yat-sen University; the Chinese Academy of Sciences (CAS) Large-Scale Scientific Facility Program; Joint Large-Scale Scientific Facility Funds of the NSFC and CAS under Contract No. U1832207; the CAS Center for Excellence in Particle Physics (CCEPP); 100 Talents Program of CAS; The Institute of Nuclear and Particle Physics (INPAC) and Shanghai Key Laboratory for Particle Physics and Cosmology; ERC under Contract No. 758462; European Union's Horizon 2020 research and innovation program under Marie Sklodowska-Curie Grant Agreement under Contract No. 894790; German Research Foundation DFG under Contract No. 443159800, Collaborative Research Center CRC 1044, GRK 2149; Istituto Nazionale di Fisica Nucleare, Italy; Ministry of Development of Turkey under Contract No. DPT2006K-120470; National Science and Technology fund; National Science Research and Innovation Fund (NSRF) via the Program Management Unit for Human Resources & Institutional Development, Research and Innovation under Contract No. B16F640076; STFC (United Kingdom); Suranaree University of Technology (SUT), Thailand Science Research and Innovation (TSRI), and National Science Research and Innovation Fund (NSRF) under Contract No. 160355; The Royal Society, UK under Contracts No. DH140054, No. DH160214; The Swedish Research Council; U.S. Department of Energy under Contract No. DE-FG02-05ER41374.

[1] F.-S. Yu, H.-Y. Jiag, R.-H. Li, C.-D. Lü, W. Wang, and Z.-X. Zhao, Chin. Phys. C **42**, 051001 (2018).
[2] R. Dutta, Phys. Rev. D **93**, 054003 (2016).
[3] W. Detmold, C. Lehner, and S. Meinel, Phys. Rev. D **92**, 034503 (2015).
[4] H. Y. Cheng, Chin. J. Phys. **78**, 324–362 (2022).
[5] G. S. Abrams *et al.*, Phys. Rev. Lett. **44**, 10 (1980).
[6] M. Ablikim *et al.* (BESIII Collaboration), Phys. Rev. Lett. **128**, 142001 (2022).
[7] J. Adler *et al.*, Phys. Rev. Lett. **62**, 1821 (1989).
[8] M. Ablikim *et al.* (BESIII Collaboration), Phys. Rev. Lett. **118**, 112001 (2017).
[9] M. Ablikim *et al.* (BESIII Collaboration), Chin. Phys. C **47**, 023001 (2023).
[10] M. Ablikim *et al.* (BESIII Collaboration), Phys. Lett. B **772**, 388 (2017).
[11] R. L. Workman *et al.* (Particle Data Group), Prog. Theor. Exp. Phys. **2022**, 083C01 (2022).
[12] C. Q. Geng, Y. K. Hsiao, C.-W. Liu, and T.-H. Tsai, Phys. Rev. D **99**, 073003 (2019).
[13] G. D. Crawford *et al.* (CLEO Collaboration), Phys. Rev. D **45**, 752 (1992).
[14] M. Ablikim *et al.* (BESIII Collaboration), Chin. Phys. C **46**, 113002 (2022).
[15] M. Ablikim *et al.* (BESIII Collaboration), Chin. Phys. C **46**, 113003 (2022).
[16] M. Ablikim *et al.* (BESIII Collaboration), Nucl. Instrum. Methods Phys. Res., Sect. A **614**, 345 (2010).
[17] S. Agostinelli *et al.*, Nucl. Instrum. Methods Phys. Res., Sect. A **506**, 250 (2003).
[18] S. Jadach, B. F. L. Ward, and Z. Wąs, Phys. Rev. D **63**, 113009 (2001).
[19] D. J. Lange, Nucl. Instrum. Methods Phys. Res., Sect. A **462**, 152 (2001).
[20] R. G. Ping, Chin. Phys. C **32**, 599 (2008).
[21] J. C. Chen, G. S. Huang, X. R. Qi, D. H. Zhang, and Y. S. Zhu, Phys. Rev. D **62**, 034003 (2000).
[22] R. L. Yang, R. G. Ping, and H. Chen, Chin. Phys. Lett. **31**, 061301 (2014).
[23] B. Richter-Was, Phys. Lett. B **303**, 163 (1993).
[24] H. Albrecht *et al.* (ARGUS Collaboration), Phys. Lett. B **241**, 278 (1990).
[25] L. Liu, X. R. Zhou, and H. P. Peng, Nucl. Instrum. Methods Phys. Res., Sect. A **1033**, 166672 (2022).
[26] M. Ablikim *et al.* (BESIII Collaboration), Chin. Phys. C **46**, 074001 (2022).